

Granulocyte colony-stimulating factor attenuates oxidative stress–induced apoptosis in vascular endothelial cells and exhibits functional and morphologic protective effect in oxygen-induced retinopathy

Hiroshi Kojima,¹ Atsushi Otani,¹ Akio Oishi,¹ Yukiko Makiyama,¹ Satoko Nakagawa,¹ and Nagahisa Yoshimura¹

¹Department of Ophthalmology, Kyoto University Graduate School of Medicine, Kyoto, Japan

Granulocyte colony-stimulating factor (G-CSF) is a known hematopoietic glycoprotein, and recent studies have revealed that G-CSF possesses other interesting properties. Oxidative stress is involved in many diseases, such as atherosclerosis, heart failure, myocardial infarction, Alzheimer disease, and diabetic retinopathy. This study was designed to examine whether G-CSF has a protective effect on endothelial cells against oxidative stress and to investigate whether G-CSF has a therapeutic role in ischemic vascular dis-

eases. Expression of G-CSF ($P < .01$) and G-CSF receptor ($P < .05$) mRNA in human retinal endothelial cells (HRECs) was significantly up-regulated by oxidative stress. Treatment with 100 ng/mL G-CSF significantly reduced H₂O₂-induced apoptosis in HRECs from 61.7% to 41.4% ($P < .05$). Akt was phosphorylated in HRECs by G-CSF addition, and LY294002, a PI3K inhibitor, significantly attenuated the antiapoptotic effect of G-CSF (by 44.1%, $P < .05$). The rescue effect was also observed in human umbilical vein

endothelial cells. In mouse oxygen-induced retinopathy model, G-CSF significantly reduced vascular obliteration ($P < .01$) and neovascular tuft formation ($P < .01$). G-CSF treatment also clearly rescued the functional and morphologic deterioration of the neural retina. A possibility of a novel therapeutic strategy for ischemic diseases through attenuating vascular regression using G-CSF was proposed. (*Blood*. 2011;117(3):1091-1100)

Introduction

Ischemic retinal diseases, such as retinal vein occlusion, diabetic retinopathy (DR), and retinopathy of prematurity (ROP), are major causes of severe visual loss in developed countries, and they should be overcome. DR is a common and important complication of diabetes mellitus (DM) that can eventually result in blindness. DR is one of the microvascular diseases, and most of its pathologic features are the result of changes in retinal microvasculature. One of the earliest DR-related events involves pericyte loss and thickening of basement membrane of the vasculature. These changes result in breakdown of the blood-retinal barrier and cause many typical clinical changes, including edema in the neurosensory retina. DR can further progress into a severe stage. In proliferative DR, new blood vessels develop with fibroglial and fibrovascular proliferation, resulting in uncontrollable tractional retinal detachment and hemorrhage. The earliest pathologic proliferative DR-related event involves lack of oxygen in the retina caused by the formation of avascular retinal nonperfusion and, thus, loss of endothelial cells.^{1,2} Apoptosis may play a crucial role in the development of DR-related microvascular cell loss^{3,4}; however, the biochemical and molecular mechanisms of endothelial cell loss in DR are not well understood.

Hyperglycemia is considered to be a major risk factor for retinal microvascular cell loss in DR, and studies have suggested that oxidative stress is one of the key players in the pathology of hyperglycemic damage. Hyperglycemia directly or indirectly induces apoptosis of microvascular cells,^{1,4-6} and oxidative stress induces apoptosis of vascular cells under hyperglycemic condi-

tions.^{6,7} Hyperglycemia generates reactive oxygen species and causes development of DR.^{8,9} Oxidative stress is increased in the diabetic retina, and the use of antioxidants inhibits cell death in retinal capillary cells.¹⁰ These studies suggest that oxidative stress is a key factor in the development of DR and that management of oxidative stress-induced vascular cell damage might be a therapeutic strategy in DR prevention.

Granulocyte colony-stimulating factor (G-CSF) is a glycoprotein commonly used in clinics to treat neutropenia and is known to mobilize bone marrow (BM)-derived hematopoietic cells into the peripheral blood. In addition to these hematopoietic effects, G-CSF has other interesting properties, including protective effects in particular cell types, such as neural cells and muscular cells as observed in cerebral damage models¹¹⁻¹⁴ and in myocardial infarction.¹⁵⁻¹⁷ We recently detected the existence of G-CSF receptors (G-CSFRs) in the retina and demonstrated the neuroprotective effect of G-CSF in retinal photoreceptor cells.¹⁸ Although G-CSF stimulates angiogenic functions in mature endothelial cells through enhanced migration, proliferation, and tube formation in vitro,^{19,20} no studies have examined the protective effect of G-CSF in vascular endothelial cells.

This study was designed to investigate the potential of G-CSF as a therapeutic candidate in preventing retinal ischemic vascular diseases, such as DR. We found that G-CSF attenuated oxidative stress-induced apoptosis in human retinal endothelial cells (HRECs) and had a protective role in the mouse model of ischemic retinopathy.

Submitted May 22, 2010; accepted October 19, 2010. Prepublished online as *Blood* First Edition paper, November 8, 2010; DOI 10.1182/blood-2010-05-286963.

The online version of this article contains a data supplement.

The publication costs of this article were defrayed in part by page charge payment. Therefore, and solely to indicate this fact, this article is hereby marked "advertisement" in accordance with 18 USC section 1734.

© 2011 by The American Society of Hematology

Methods

Cell culture

The cell lines (HRECs) were obtained from Applied Cell Biology Research Institute. The cells were grown in Cell Systems Corporation complete medium kit (DS Pharma Biomedical) based on a basal Dulbecco modified Eagle medium and F12 medium (1:1) supplemented with 10% fetal bovine serum and 1% penicillin/streptomycin.

The cells were incubated in 95% air and 5% CO₂ at 37°C, and the media was changed every 7 days until the cells grew to 80% confluence. Passages 4 to 8 were used in the experiments. The cells were starved for 18 hours with serum-free CS-C medium before treatment. Recombinant human G-CSF 10 to 1000 ng/mL (Kirin) was added to the cells and incubated for 24 hours before exposure to oxidative damage. Blocking of intracellular signaling was performed by adding 100nM AG 490 (Calbiochem), an inhibitor of JAK2, or 10 μ M LY294002 (SA Biosciences), an inhibitor of PI3K, with G-CSF treatment. We have tested several different concentrations in previous studies,^{21,22} and the concentration used in this study was based on this.

Oxidative damage

Oxidative damage was induced by adding H₂O₂ as described previously.²⁴ After HRECs were treated with G-CSF or inhibitors for 24 hours, the culture medium was replaced with the same medium containing 1mM H₂O₂ and then incubated for another 6 to 24 hours. The cell images were taken with a microscope (Axio Imager, Carl Zeiss) and analyzed with the software provided (Axiovision Version 4.3, Carl Zeiss). The images were imported into Photoshop software (Version 10.0.1, Adobe Systems) as a series of .tif files.

Measurement of apoptosis

The number of apoptotic cells resulting from oxidative damage was measured by a system using fluorescence-activated cell sorter (FACScan with CellQuest software, Version 3.3; BD Biosciences).²⁴ Briefly, after treatment, the cells were harvested and resuspended in a binding buffer (10mM N-2-hydroxyethylpiperazine-N'-2-ethanesulfonic acid, 140mM NaCl, and 2.5mM CaCl₂; pH 7.4). Then, 100 μ L of the cell suspension was transferred to a 5-mL culture tube, to which 5 μ L of fluorescein isothiocyanate-conjugated annexin V (BD Biosciences) and 2 μ L of propidium iodide (BD Biosciences) were added. After 15 minutes of incubation in the dark at room temperature, the cells were diluted with 300 μ L of binding buffer before cytometric analysis. The samples were analyzed by fluorescence-activated cell sorter. A total of 20 000 events per sample were acquired in each experiment.

Western blot analysis

Freshly collected cells were centrifuged at 14 000g for 10 minutes at 4°C, after which the protein concentration of the supernatant was determined. Each protein sample (40 μ g) was electrophoresed on a 5% to 20% gradient gel (ATTO) and transferred to a polyvinylidene fluoride membrane (ATTO). For the G-CSFR blot, a mouse monoclonal antibody to G-CSFR (Santa Cruz Biotechnology), Phospho-Jak2 blot, a rabbit polyclonal antibody to Phospho-Jak2 (Cell Signaling Technology), and a goat antirabbit IgG antibody conjugated with horseradish peroxidase (Vector Laboratories) were used. The antibodies used were Jak2 antibody, Phospho-stat3 antibody, Stat3 antibody, Phospho-Akt antibody, and Akt antibody (Cell Signaling Technology). Protein signals were detected by chemiluminescence (Chemi-Lumi One L, Nakarai) exposed to imaging film. For β -actin normalization, blots were reprobated with Antibeta-Actin Antibody (Cell Signaling Technology).

Reverse transcriptase-PCR

Total RNA was isolated with RNeasy (QIAGEN), treated with RNase-free DNase I, and reverse-transcribed with a first-strand cDNA synthesis kit (GE

Healthcare) according to the manufacturer's protocols. Quantitative real-time polymerase chain reaction (PCR) was performed with an ABI PRISM 7000 Sequence Detection System (Applied Biosystems). Reactions were performed in duplicate with a SYBR Green PCR Master Mix (Applied Biosystems). PCR primers for G-CSF (csf3, accession number NM_009971.1: forward, 5'-CTACAAGCTGTGTTCATCCGGAG-3'; and reverse, 3'-CATCCAGGTGAAGCATATCCAA-5'), G-CSFR (csf3r, accession number NM_007782.2: forward, 5'-TGTGCCCAACCTC-CAAACCA-3'; and reverse, 3'-GCTAGGGGCCAGAGACAGAGACAC-5'), and intrinsic control β -actin were purchased from Applied Biosystems. Cycling conditions were as follows: 10 minutes at 95°C, 15 seconds at 95°C, and 1 minute at 60°C for 40 cycles. Amplification plots and cycle threshold values from the exponential phase of the PCR were analyzed with ABI Prism SDS, Version 1.7 software (Applied Biosystems). Relative regulation levels were determined after normalization to β -actin.

OIR model

Animals were always treated according to the Association for Research in Vision and Ophthalmology Statement for the Use of Animals in Ophthalmic and Vision Research and the Guideline for Animal Experiments of Kyoto University. All animals were obtained from Japan SLC and housed in the Institute of Laboratory Animals Graduate School of Medicine of Kyoto University. Oxygen-induced retinopathy (OIR) was induced in newborn C57BL/6 mice as described by Smith et al²⁵ Briefly, on postnatal day 7 (P7), newborn mice were placed along with their dams into 75% oxygen. After 5 days, on P12, they were transferred back to room air. During the period, room temperature was maintained at 20°C, and illumination was provided by standard fluorescent lighting on a 12-hour light-dark cycle. Pups were nursed by their dams and dams were given food and water. Daily injection of G-CSF (50 μ g/kg) or vehicle continued for the following 5 days from P6 to P10. The concentration of G-CSF was determined according to experiments of the previous study.²⁶ Intravitreal injection of G-CSF (50 μ g/kg) or vehicle was performed following a previously described method.²⁷ Briefly, mice were anesthetized, and 0.5 μ L G-CSF or vehicle was injected intravitreally using a 33-gauge needle (Hamilton).

Retinal whole-mount preparation and immunohistochemistry

Retinal whole-mount preparations were created as described previously.²⁸ Briefly, mice retinas were harvested and fixed with ice-cold 4% paraformaldehyde and methanol, followed by blocking with 50% fetal bovine serum and 20% normal goat serum for 1 hour at room temperature. The primary antibodies used were anticollagen type IV (Chemicon) and anti-CD45 (Millipore). The secondary antibodies were Alexa 594-conjugated antibodies and Alexa 488-conjugated antibodies (Invitrogen).

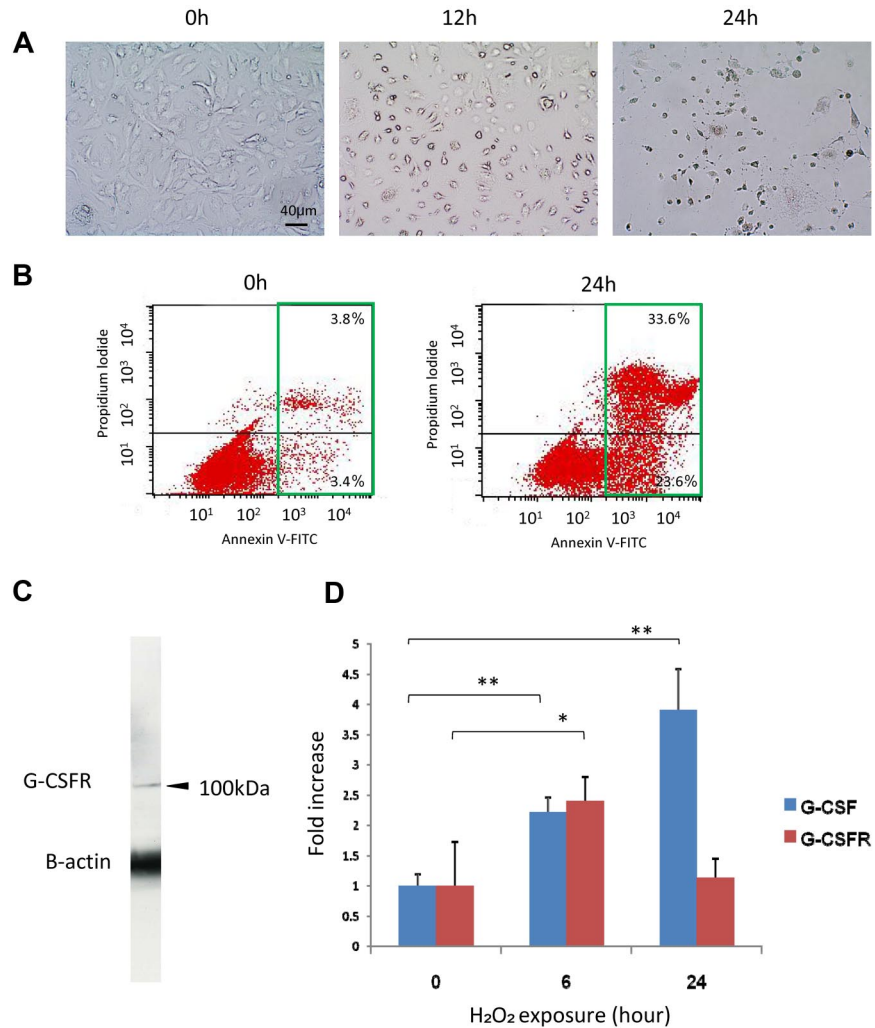
Imaging and quantifying nonperfusion and neovascular tuft areas and pan-hematopoietic cells

Retinal whole-mount images were taken with a microscope (Axio Imager, Carl Zeiss) and analyzed by the provided software (Axiovision, Version 4.3, Carl Zeiss). After montages of the retinas were created, quantification of the nonperfusions and neovascular tufts was carried out as described previously.²⁹ In short, the areas of nonperfusion and neovascular tufts were selected using Photoshop software Version 10.0.1 (Adobe) on the high-resolution image of the retinal whole-mount staining. Total areas were expressed in pixels and then converted to square micrometers. The conversion factor was calculated to be 32.17 μ m²/pixel for our experiment. The number of pan-hematopoietic cells in the retina was speculated by counting CD45⁺ cells.

ERGs

After overnight dark adaptation, mice were anesthetized and their pupils were fully dilated with medication. During the record, mice were kept on a heating pad to maintain body temperature. Electroretinograms (ERGs) were recorded with a PowerLab 2/25 (AD Instruments) using gold wire loops placed on the right corneas. Reference electrodes were placed in the cheek and ground leads were placed in the hip.

Figure 1. H₂O₂ induced apoptosis and increased G-CSF and G-CSFR expression in HRECs. (A) Representative images of H₂O₂-induced apoptosis in HREC culture. Note that the number of apoptotic cells increased with time. h indicates hours after exposure to H₂O₂. (B) The number of apoptotic cells was measured by fluorescence-activated cell sorter using annexin V antibody. Increases in the number of annexin V-positive cells at 24 hours (green square) were observed. Note that numbers of both the early apoptotic cells (bottom right quadrant) and the late apoptotic or necrotic cells (top right quadrant) were increased by H₂O₂. (C) G-CSFR expression on HRECs was confirmed by Western blot analysis. (D) The effect of oxidative stress on G-CSFR or G-CSF mRNA expression in HRECs. Expression of G-CSF mRNA was significantly increased over time by oxidative stress (n = 4 at each point). ***P* < .01. Increased G-CSFR mRNA expression was observed at 6 hours after 1mM H₂O₂ exposure (n = 4 at each point), and the level was returned to normal at 24 hours. **P* < .05.



Full-field scotopic ERGs were measured by 3-ms flashes at an intensity ranging from 0.002 to 30 cd-s/m² at 1-minute intervals without averaging of the multiple responses. Subsequently, photopic ERGs were recorded at an intensity ranging from 3.288 to 30 cd-s/m² flash and with 30 cd/m² background light after 7-minute light adaptation, filtered between 0.3 and 500 Hz, and stored. During the recording of photopic ERGs, 32 measurements were obtained and averaged.

For statistical analysis, scotopic ERGs recorded at intensities of 0.0127, 0.3279, 3.288, and 30 cd-s/m² and photopic ERGs at intensities of 3.288 and 30 cd-s/m² were used. Amplitudes of the a-waves were measured from the baseline to the peak in the cornea-negative direction; b-waves were measured from the cornea-negative peak to the major cornea-positive peak. Photopic peak responses were measured from the baseline to the maximum cornea-positive peak. These analyses were performed using SCOPE 3, Version 3.8.2 software (AD Instruments).

Histologic analysis

After ERGs were recorded, the mice were transcardially perfused with 4% paraformaldehyde (Wako) and 0.25% glutaraldehyde (Wako). The eyes were enucleated, fixed with the same solution, and embedded in paraffin, and 2-μm-thick vertical sections were made through the optic discs. These specimens were stained with hematoxylin and eosin, observed, and photographed with a microscope (Axio Imager). The images were imported into Photoshop software (Version 10.0.1, Adobe Systems) as a series of .tif files. Measurements of retinal layer thickness were performed using specimens from the same area of the retina (500 μm and 1000 μm from each optic disc), and the values of both eyes were averaged and used as one sample for statistical analysis.

Statistical analysis

All results for continuous variables are expressed as the mean plus or minus SEM. Data between each group were compared using one-way analysis of variance followed by Bonferroni correction. A *P* value less than .05 was considered statistically significant. All analyses were performed using SPSS, Version 13.0 software.

Results

Oxidative stress induced the expression of G-CSF and G-CSFR mRNA in HRECs

Among the conditions tested, we found that 24-hour exposure to 1mM H₂O₂ was the best for further experiments that induced apoptosis in around 60% of the HRECs (Figure 1A-B). Thus, the experiments with HRECs in this study were done under those conditions unless otherwise indicated.

Expression of G-CSFRs on human umbilical vein endothelial cells has been shown previously. We also confirmed by Western blot analysis (Figure 1C) and PCR (Figure 1D) that G-CSFRs are expressed in HRECs. Expression of G-CSF mRNA was significantly induced by oxidative stress, 2.2- plus or minus 0.2-fold (*P* < .01) at 6 hours and 3.9- plus or minus 0.7-fold (*P* < .01) at 24 hours (Figure 1D). Increased G-CSFR mRNA expression was observed at 6 hours (2.4 ± 0.4-fold, *P* < .05) but returned to

normal level at 24 hours (Figure 1D). These data suggested that the G-CSF/G-CSFR system may possibly have some role against oxidative stress in HRECs. In addition, the expression of G-CSF on human RPE cells was also dramatically induced by oxidative stress (data not shown).

G-CSF reduces oxidative stress–induced apoptosis on HRECs and human umbilical vein endothelial cells

We examined whether G-CSF confers direct protective effect on HRECs in the same way that it prevents apoptotic death in myocardial cells.³⁰ Treatment with G-CSF reduced H₂O₂-induced apoptosis in HRECs in a dose-dependent manner (Figure 2A-B). A 24-hour H₂O₂ exposure induced apoptosis in 61.7% of HRECs, and 10, 100, and 1000 ng/mL G-CSF treatment reduced the rate of apoptosis to 48.9%, 41.4%, and 48.3%, respectively ($P < .05$ for 100 ng/mL; Figure 2B). G-CSF (100 ng/mL) treatment also showed significant rescue effect in H₂O₂ exposed human umbilical vein endothelial cells ($P = .01$, data not shown).

The G-CSF antiapoptotic pathway has been reported through JAK/STAT in neutrophilic granulocytes^{31,32} and through PI3K-Akt signaling activation in neuronal cells.^{26,33} AG 490, a JAK2 inhibitor, did not alter the G-CSF-mediated antiapoptotic effect in HRECs; however, treatment with LY294002, a PI3K inhibitor, significantly attenuated the antiapoptotic effect by 82.9% ($P < .05$, Figure 2C). Only Akt, but not JAK2, STAT3 (Figure 2D), or MEK/ERK (supplemental Figure 1, available on the *Blood* Web site; see the Supplemental Materials link at the top of the online article), was phosphorylated on addition of G-CSF. This finding suggested that the PI3K-Akt pathway has a major role in the G-CSF-mediated protective effect on HRECs.

G-CSF attenuated oxygen-induced regression of the retinal vasculature in the mouse OIR model

Apoptosis of vascular endothelial cells resulting in vascular regression is considered a major early pathology in DR. Hyperglycemia-induced oxidative stress is one of the major triggers of apoptosis.^{4,6,7} Thus, blocking oxidative stress-induced apoptosis of retinal endothelial cells might be a promising therapeutic strategy for DR. To investigate whether G-CSF is a potential therapeutic strategy, a mouse model of OIR that has been shown to have an important role in vascular regression³⁴⁻³⁶ was used. The OIR model is also an important model of angiogenesis, a major pathology of progressed DR. We scheduled a daily intraperitoneal injection of G-CSF between P6 and P10 (Figure 3A).

High oxygen exposure from P7 to P12 resulted in a significant retinal capillary drop, especially at the central area at P12 (Figure 3B-C). After the mice were back on normal air, new vessels grew from the superficial plexus at the transition between the perfusion and nonperfusion areas and extended to the central avascular areas (Figure 3E). G-CSF resulted in a significant reduction of the vascular obliteration area at P12 compared with vehicle-treated controls (G-CSF-treated, $3\,819\,139 \pm 625\,296 \mu\text{m}^2$; vehicle-treated; $4\,605\,728 \pm 697\,644 \mu\text{m}^2$; $P < .01$; Figure 3C-D,G). Furthermore, the area of vascular obliteration measured at P17 was still significantly reduced in G-CSF-treated retinas (G-CSF-treated; $254\,248 \pm 278\,656 \mu\text{m}^2$; vehicle-treated, $3\,056\,476 \pm 623\,587 \mu\text{m}^2$; $P < .05$; Figure 3E-F,H). A significant reduction in neovascular tuft was also observed in G-CSF-treated eyes compared with vehicle-treated controls (G-CSF-treated, $1\,210\,199 \pm 278\,656 \mu\text{m}^2$; vehicle-treated, $1\,657\,328 \pm 416\,377 \mu\text{m}^2$; $P < .01$; Figure 3E-F,I). Furthermore, we investigated the effect of direct injection of G-CSF into the eye of the

OIR model (at P6) and observed an obvious rescue effect of retinal vasculature (G-CSF-treated, $3\,505\,480 \pm 586\,891 \mu\text{m}^2$; vehicle-treated; $4\,562\,419 \pm 451\,396 \mu\text{m}^2$; $P < .05$; Figure 3J-L). Administration of G-CSF after exposure to high oxygen (P12 to P16) did not alter the vascular status of the OIR model (data not shown). Because reports have shown that direct injection of BM cells into eyes in the OIR model did not prevent vaso-obliteration during exposure to high oxygen levels between P7 and P12,²⁹ the vaso-obliterating effect of G-CSF observed in this study might not be mediated through BM-derived cells but, rather, might work directly on the endothelial cells. We also examined the G-CSF-treated retina using an anti-CD45 antibody and found that there was no difference in the number of BM-derived hematopoietic cells between the treated and nontreated retinas in the OIR model (Figure 3M-O).

G-CSF treatment rescued the retina from hyperoxia-induced functional and morphologic damage in the OIR model

The retina is one of the most highly vascularized tissues in the body, and its vasculature contributes significantly to visual function. Indeed, irreversible functional and morphologic damage to the retina was often observed clinically in DR and ROP, even after clinical remission.³⁷⁻³⁹ In a rat OIR model, exposure to hyperoxia resulted in reduction of the amplitude in ERG and thinning of the outer plexiform layer (OPL).⁴⁰ Thus, we concluded that the OIR model is a clinically relevant model for assessing irreversible neural damage caused by oxidative damage observed in human DR and ROP.

To investigate whether G-CSF treatment has the potential to attenuate permanent damage to the retina, electrophysiologic and morphologic analyses of the retinas at P30 were performed. In control mice, amplitudes obtained from the retina increased according to the increases in light intensity. Mice treated with high levels of oxygen showed significant decreases in both a-wave and b-wave amplitude, and G-CSF treatment significantly reduced the amplitude decreases in all light intensities (Figures 4A-D). A similar significant rescue effect of G-CSF was observed in both photopic and scotopic conditions. Furthermore, G-CSF shortened implicit times of a-wave and b-wave (Figure 4E-G). OPLs were clearly thinner and disorganized in OIR mice compared with control mice, and G-CSF treatment partially but significantly attenuated OPL changes throughout the retina (Figure 5A-B). These data suggest that G-CSF has a therapeutic potential for preventing oxidative stress-induced irreversible functional and morphologic damage. The thickness of the outer segment (OS), but not outer nuclear layer, was decreased in the OIR model compared with that of the control, and G-CSF had no detectable effect on these layers (Figure 5C-D).

Changes of G-CSF and G-CSFR expression in retinas of the OIR model

G-CSFR mRNA expression was increased with age by P8 in wild-type mice. Exposure to high oxygen further increased G-CSFR expression (maximum of 2.4-fold at P12, $P < .05$), which gradually decreased to normal levels after the mice were returned to normal air (Figure 6A). In contrast, exposure to high oxygen levels reduced age-dependent G-CSF increases (45.2% at P12, $P < .05$), which returned to normal levels by P30 (Figure 6B). Furthermore, G-CSF was significantly up-regulated even in wild-type adult mouse retinas exposed to high levels of oxygen (reverse-transcribed PCR, 3.7-fold, $P < .05$, data not shown). These data suggest the existence of endogenous oxygen responsive

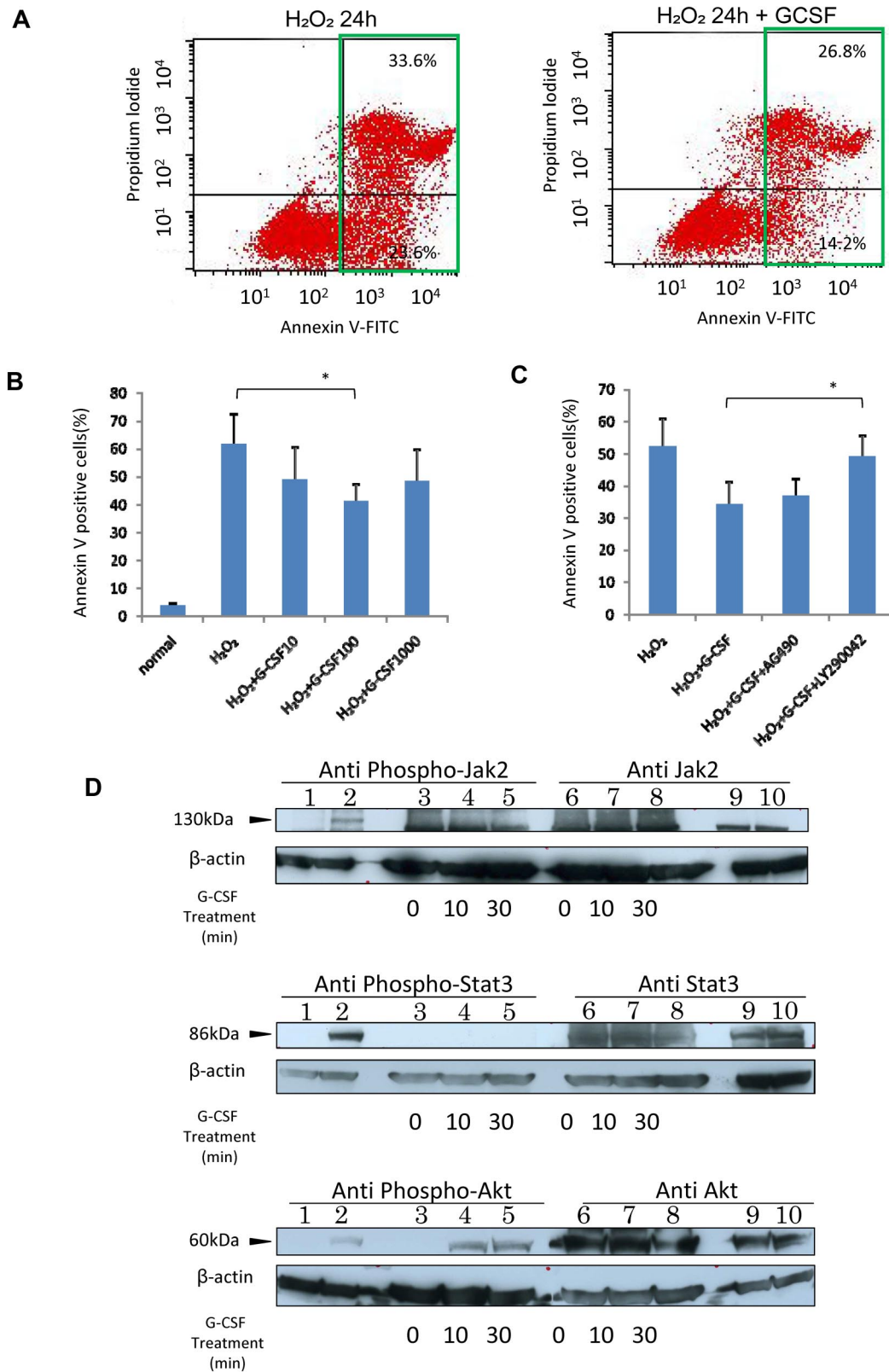


Figure 2. G-CSF protected HRECs from oxidative stress-induced apoptosis through the PI3K-Akt pathway. (A) Left panel: The result of 24-hour exposure to 1mM H₂O₂; and the right panel, results of G-CSF addition. Note the decreased numbers of apoptotic cells (green squares) in the G-CSF-treated group. (B) Dose-dependent antiapoptotic effect of G-CSF. Cells were incubated with G-CSF (10, 100, or 1000 ng/mL) for 24 hours followed by exposure to 1mM H₂O₂ for another 24 hours. The maximum effect was observed with 100 ng/mL G-CSF (n = 6 at each point). *P < .05. (C) The rescue effect of 100 ng/mL G-CSF was attenuated by LY294002 (n = 6 at each point) but not by AG490. *P < .05. (D) Intracellular Jak2 (upper panel), stat3 (middle panel), and Akt (lower panel) phosphorylation profiles in G-CSF-activated HRECs. Lanes 1, 2, 9, and 10 are controls: lane 1, nonphosphorylated cell extracts; lane 2: phosphorylated cell extracts; and lane 9: phosphorylated cell extracts. Lanes 3 to 8: HREC lysates, 20 μg per lane treated for 0 minutes (untreated, lanes 3 and 6), 10 minutes (lanes 4 and 7), and 30 minutes (lanes 5 and 8) with 100 ng/mL G-CSF. Only Akt was phosphorylated by G-CSF in HRECs, and the result was concordant with the results of the blocking experiments.

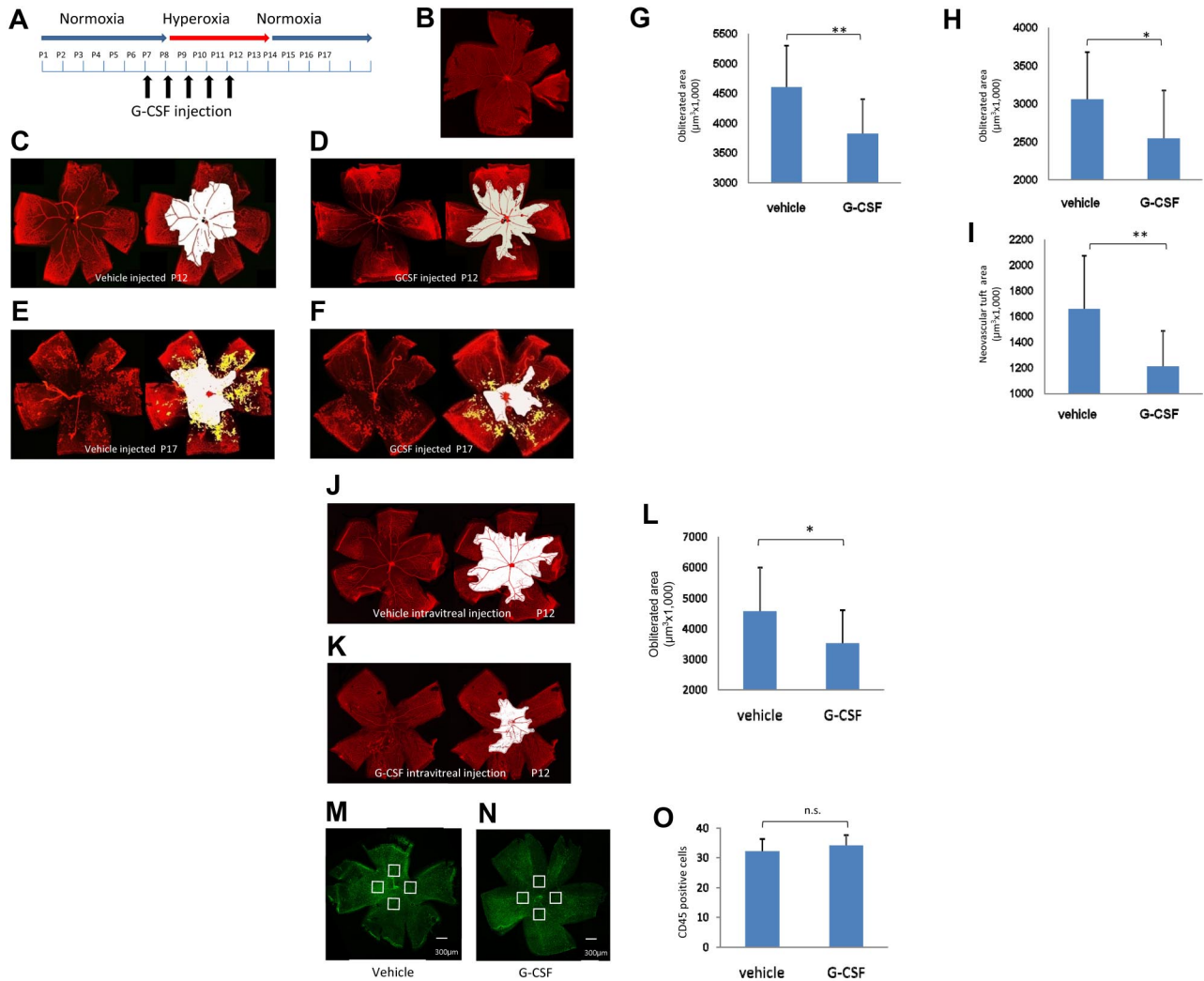


Figure 3. G-CSF rescued the vascular change in the OIR model. (A) Time scheme of the experiments. G-CSF (50 μg/kg) was administered intraperitoneally daily between P6 and P10. (B-F) Retinal whole mounts stained with collagen IV antibody to detect the area with retinal vasculature. (B-C) Control P7 and P12, respectively. Note the nonvascular area (white) in the P12 retina that was not observed in the P7 retina. Vascular obliteration occurred between P7 and P12 in this model. (D) A G-CSF-treated P12 retina. The area of vascular obliteration (white) was decreased by G-CSF. (E-F) At P17, neovascular tufts (yellow) and vascular attenuation (white) were marked in the control OIR retina (E), and G-CSF reduced both changes (F). (G) G-CSF injection reduced the obliteration area at P12 compared with the control (n = 13 each group). ** $P < .01$. (H-I) G-CSF reduced both the vascular obliterated area and the neovascular tuft at P17 compared with the controls (n = 13 in each group). * $P < .05$. ** $P < .01$. (J-L) Intravitreal injection of G-CSF (P6) also reduced the vascular attenuation (white) in the OIR model. (J) Control treated retina at P12. (K) G-CSF-treated retina at P12. Intravitreal G-CSF injection reduced the obliteration area significantly to that of control (n = 5 each group). * $P < .05$. (M-O) Vehicle-treated (M) and G-CSF-treated (N) OIR retina, stained with CD45 antibody, and counted the CD45⁺ cells at 4 points of 300 μm² in the avascular area at P12. No remarkable difference in the number of CD45⁺ cells. (O) n = 4 each group. $P > .05$.

G-CSF/G-CSFR system in the retina. Although up-regulated G-CSF might have many roles, our results suggested that one of them is a protective role against retinal injury.

Discussion

This study is the first to evidence that G-CSF has an antiapoptotic effect on vascular endothelial cells and can protect the retina from oxidative stress-induced pathologic damage. The findings suggest a novel treatment strategy for oxidative stress-induced retinal diseases, such as DR or ROP, by preventing vascular dropout using medicine that is already available in clinics.

Current strategies for DR were developed to prevent pathologic neovascularization. Laser photocoagulation is used to make chorioretinal scars, which controls the retinopathy. Recently developed antivascular endothelial growth factor was also designed to prevent

retinal neovascularization. However, in many DR cases, retinal function is irreversibly deteriorated after formation of avascular retinal areas and sufficient visual function cannot be achieved even after successful treatment. Functional deterioration should be prevented to achieve sufficient visual function, and preventing the formation of avascular retinal areas might be one of the best strategies for the purpose.

G-CSF is a powerful cytokine that induces mobilization of hematopoietic stem cells (HSCs) into the peripheral circulation. It is commonly used in clinical practice for the adoption of autologous peripheral blood stem cell transplantation. In addition to its hematopoietic effect, recent studies have revealed that G-CSF possesses other interesting effects. The antiapoptotic effect of G-CSF has been shown in several cell types, including cardiomyocytes and neuronal cells.¹¹⁻¹⁴ G-CSF has a role in myocardial regeneration and induction of angiogenesis in ischemic diseases.^{15-17,41} Clinical application of G-CSF has been already investigated for the

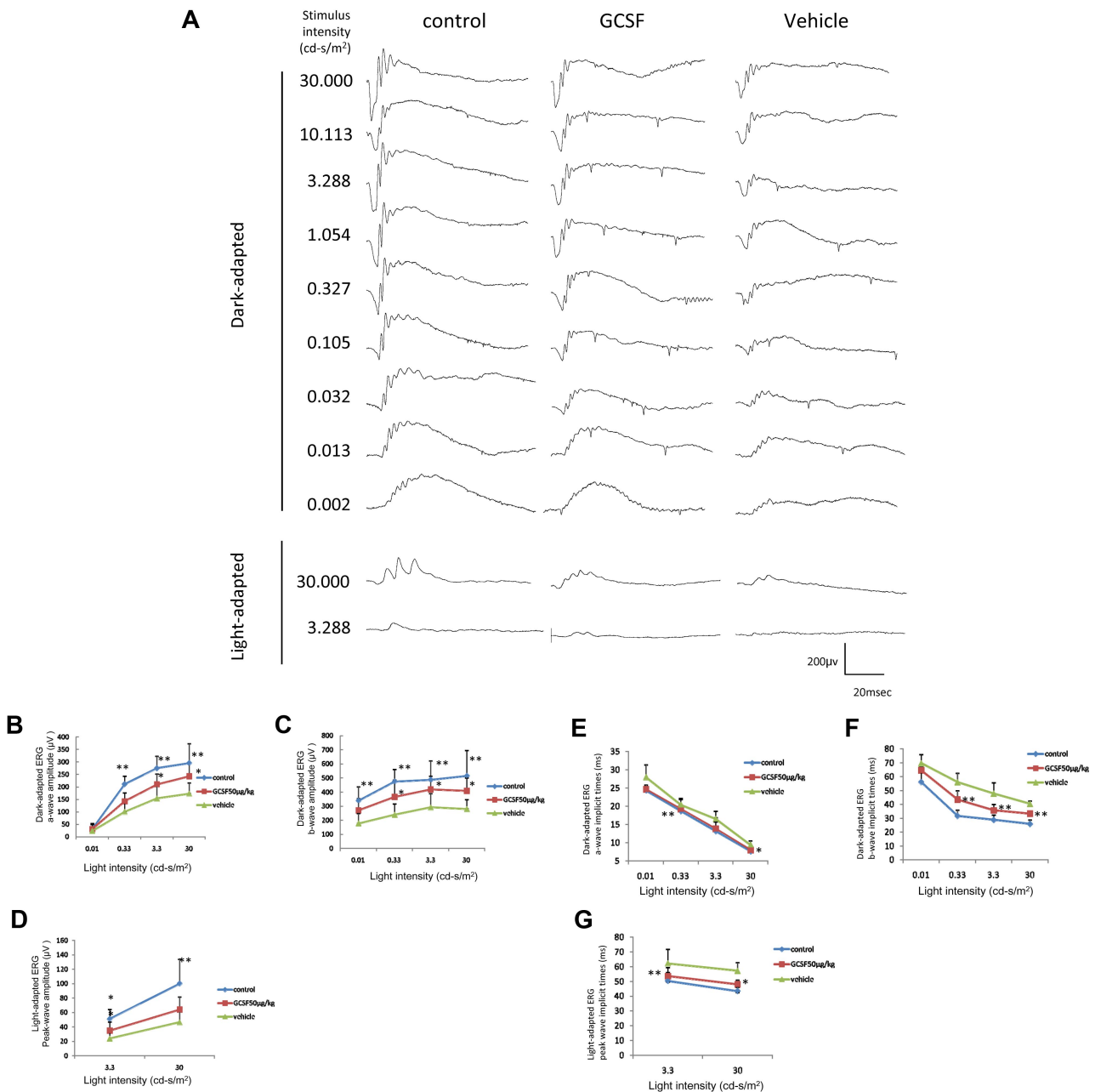


Figure 4. Functional rescue of G-CSF in the OIR model. (A) Representative results of scotopic and photopic ERG measured at P30. Left lane: normal untreated mouse; middle lane: G-CSF (50 µg/kg)-treated OIR mouse; and right lane: vehicle-treated OIR mouse. (B-G) Quantitative results of each scotopic and photopic ERG component. ERG amplitudes and implicit times were retained in G-CSF-treated mice compared with the vehicle-treated mice (n = 10 in each group). *P < .05. **P < .01.

treatment of myocardial infarction.^{15,42,43} G-CSF was also shown to increase the efficiency of generating cardiomyocytes from embryonic stem cells, and its possible application in regenerative medicine is under investigation.⁴⁴ In the retina, similar to other neurotrophic factors, expression of G-CSF is up-regulated by injury,⁴⁵ and G-CSF has a direct neuroprotective effect and might be one of the endogenous neurotrophic factors in the retina.¹⁸ In the present study, we found a new function of G-CSF, an antiapoptotic effect in vascular endothelial cells. Because G-CSF and G-CSFR were both up-regulated in response to oxidative stress, it is possible that the G-CSF/G-CSFR system has a role of endogenous protection against oxidative stresses in HRECs.

In this study, administration of G-CSF successfully attenuated retinal vascular regression and reduced pathologic damage to the retina both morphologically and functionally in the OIR model. It

is possible that G-CSF mobilized BM-derived HSCs into the peripheral circulation and that those HSCs promoted the protective effect in the OIR model because Ritter et al reported that transplanted BM-derived progenitors dramatically accelerated retinal vascular repair in an OIR model.²⁹ To investigate the possibility of HSC participation, G-CSF was administered after exposure to hyperoxia (from P12 to P16) followed by evaluation of the vasculature at P17 to determine whether G-CSF accelerated retinal vascular repair as the BM-derived progenitors did.²⁹ Although G-CSF treatment increased the function or number of peripheral blood BM-derived progenitors (examined by the colony-forming unit of granulocyte macrophages and endothelial cells; data not shown), the retinal vasculature did not change compared with the vehicle-treated controls. Furthermore, direct injection of BM-derived progenitors did not prevent vaso-obliteration during exposure to

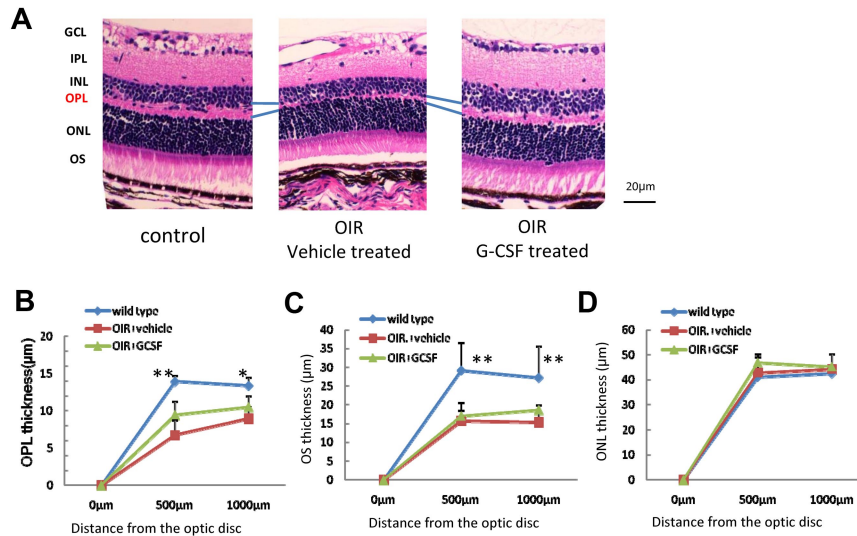


Figure 5. G-CSF attenuates OPL thinning in OIR retinas. (A) Left panel: untreated control mouse retina; middle panel: G-CSF–treated mouse retina; right panel: vehicle-treated mouse retina. (B–D) Quantitative analysis. G-CSF–treated mice had thicker OPL than did vehicle-treated mice (n = 8 in each group). **P* < .05. ***P* < .01. OIR mice had thinner OS than control mice. ***P* < .01. The OS thickness did not change by treatment (C). Outer nuclear layer (ONL) of OIR was same as control mice (D).

high oxygen levels between P7 and P12,²⁹ suggesting that BM-derived progenitors do not have an antiapoptotic effect on vascular endothelial cells in the OIR model. Because oxidative stress has an important role in the vascular regression in the OIR model,^{5,8–10} we considered that the direct antiapoptotic effect of G-CSF on HREC that was seen in the in vitro experiments was one possible mechanism underlying the G-CSF rescue effect in the OIR model.

Diabetic complications of the retina include both retinopathy and neuropathy. The term diabetic neuropathy is used to describe DM-associated neuropathic disorders. One important mechanism of diabetic neuropathies is damage to the microvasculature that supplies nervous system, and neuronal ischemia is a characteristic feature of diabetic neuropathy. At present, vascular problems in DR, including retinal neovascularization, can be managed relatively well by laser photocoagulation, antiangiogenic medicine, or surgical procedures. On the other hand, irreversible visual function loss even after the retinopathy has settled is not rare, and this is one of the most important clinical problems of DR that should be solved. In this study, G-CSF treatment demonstrated significant neuroprotective ef-

fects in addition to vascular rescue in the OIR model. Although we could not conclude that the neuroprotective effect of G-CSF in the OIR model was solely mediated through vascular protection because the direct neuroprotective effect of G-CSF has been reported by us and elsewhere,^{11–15,18} the vasculoprotective and neuroprotective role of G-CSF is very convenient as a therapeutic strategy for DR.

In the OIR model, the most impressive change is retinal vascular obliteration followed by neovascularization. It is known that the retinal vasculature mainly supplies the inner part of the retina rather than the outer retina; therefore, cellular damage may be more prominent in the inner retinal layers. Indeed, thinning of OPL is one of the most prominent histologic changes in the OIR model. In addition to OPL, OS seemed to be damaged in the OIR model (Figure 5C), but G-CSF treatment did not alter the thickness of OS. These data suggest that the effect of G-CSF was stronger in the inner layer than in the outer layer of the retina. Although histologic evaluation failed to detect these changes, functional evaluation using ERG revealed that G-CSF administration clearly attenuated retinal damage in

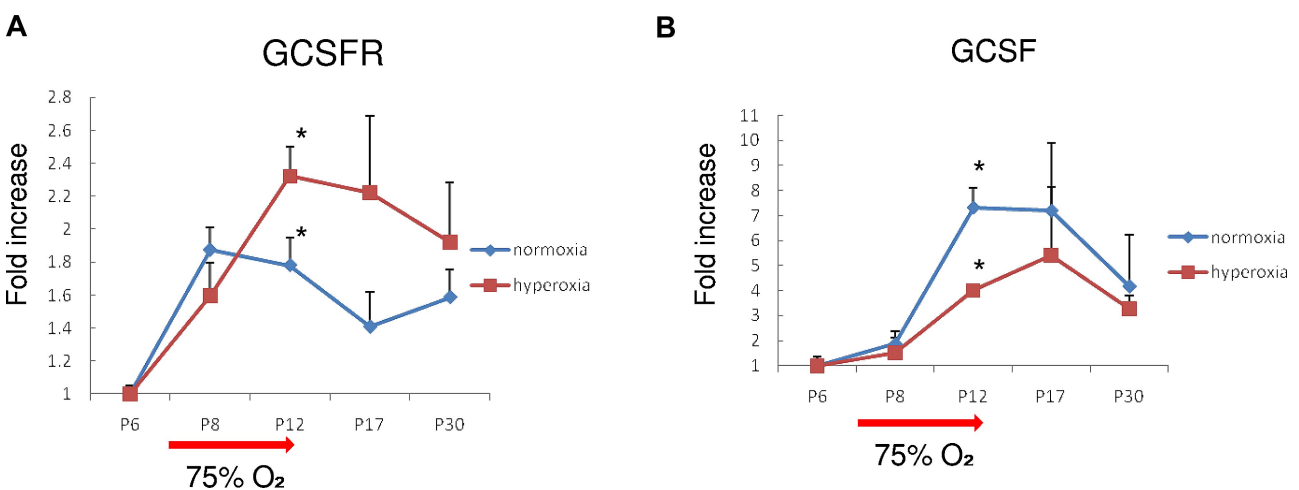


Figure 6. Expression of G-CSF and G-CSFR mRNA in normal and OIR mouse retinas. (A) The level of G-CSFR mRNA was increased by high oxygen exposure and returned to normal levels. (B) In contrast, G-CSF levels were reduced by high oxygen exposure. **P* < .05.

all layers (Figure 4). We could not investigate the effect of G-CSF for the choroidal circulation and the neural cells that are covered by choroidal circulation because we could not evaluate the change in the choroidal circulation in OIR model. Considering these results, we cannot conclude whether G-CSF directly or indirectly protected all layers of the retina in our study. Thus, we hypothesized in the manuscript that the effect of G-CSF might be mediated through both vascular and neuroprotective effects.

In conclusion, we demonstrated that G-CSF has a direct protective effect on the vascular endothelial cells and that it rescues the cells from oxidative stress-induced apoptosis. The effect, probably in conjunction with its neuroprotective effect on the retina, reduced the pathologic change in the clinically relevant disease model both morphologically and functionally. Because the G-CSF/G-CSFR system exists in the retina and seems to have an endogenous role in pathologic conditions, there may be fewer problems with its clinical application. Although there are limitations in this study, such as the clinical relevancy of the model used, we conclude that preventing retinal vascular regression with medication may be practical and might be a novel therapeutic strategy for retinal ischemic diseases, including DR. G-CSF is one such therapeutic candidate, and further investigation is underway.

References

- Diabetes Control and Complications Trial Research Group. The effect of intensive treatment of diabetes on the development and progression of long-term complications in insulin-dependent diabetes mellitus. *N Engl J Med*. 1993;329(14):977-986.
- UK Prospective Diabetes Study Group. Intensive blood-glucose control with sulphonylureas or insulin compared with conventional treatment and risk of complications in patients with type 2 diabetes (UKPDS 33). *Lancet*. 1998;352(9131):837-853.
- Allen DA, Yaqoob MM, Harwood SM. Mechanisms of high glucose-induced apoptosis and its relationship to diabetic complications. *J Nutr Biochem*. 2005;16(12):705-713.
- Mizutani M, Kern TS, Lorenzi M. Accelerated death of retinal microvascular cells in human and experimental diabetic retinopathy. *J Clin Invest*. 1996;97(12):2883-2890.
- Geraldes P, Hiraoka-Yamamoto J, Matsumoto M, et al. Activation of PKC-delta and SHP-1 by hyperglycemia causes vascular cell apoptosis and diabetic retinopathy. *Nat Med*. 2009;15(11):1298-1306.
- Busik JV, Mohr S, Grant MB. Hyperglycemia-induced reactive oxygen species toxicity to endothelial cells is dependent on paracrine mediators. *Diabetes*. 2008;57(7):1952-1965.
- Baynes JW. Role of oxidative stress in development of complications in diabetes. *Diabetes*. 1991;40(4):405-412.
- Brownlee M. Biochemistry and molecular cell biology of diabetic complications. *Nature*. 2001;414(6865):813-820.
- Cui Y, Xu X, Bi H, et al. Expression modification of uncoupling proteins and MnSOD in retinal endothelial cells and pericytes induced by high glucose: the role of reactive oxygen species in diabetic retinopathy. *Exp Eye Res*. 2006;83(4):807-816.
- Kowluru RA. Diabetic retinopathy: mitochondrial dysfunction and retinal capillary cell death. *Antioxid Redox Signal*. 2005;7(11):1581-1587.
- Schabitz WR, Kollmar R, Schwaninger M. Neuroprotective effect of granulocyte colony-stimulating factor after focal cerebral ischemia. *Stroke*. 2003;34(3):745-751.
- Gibson CL, Bath PM, Murphy SP. G-CSF reduces infarct volume and improves functional outcome after transient focal cerebral ischemia in mice. *J Cereb Blood Flow Metab*. 2005;25(4):431-439.
- Gibson CL, Jones NC, Prior MJ, Bath PM, Murphy SP. G-CSF suppresses edema formation and reduces interleukin-1beta expression after cerebral ischemia in mice. *J Neuropathol Exp Neurol*. 2005;64(9):763-769.
- Komine-Kobayashi M, Zhang N, Liu M, et al. Neuroprotective effect of recombinant human granulocyte colony-stimulating factor in transient focal ischemia of mice. *J Cereb Blood Flow Metab*. 2006;26(3):402-413.
- Kang HJ, Kim HS, Zhang SY, et al. Effects of intracoronary infusion of peripheral blood stem-cells mobilised with granulocyte-colony stimulating factor on left ventricular systolic function and restenosis after coronary stenting in myocardial infarction: the MAGIC cell randomised clinical trial. *Lancet*. 2004;363(9411):751-756.
- Ince H, Petzsch M, Kleine HD, et al. Prevention of left ventricular remodeling with granulocyte colony-stimulating factor after acute myocardial infarction: final 1-year results of the front-integrated revascularization and stem cell liberation in evolving acute myocardial infarction by granulocyte colony-stimulating factor (FIRST-LINE-AMI) trial. *Circulation*. 2005;112(9):173-180.
- Zohlhofer D, Ott I, Mehili J, et al. Stem cell mobilization by granulocyte colony-stimulating factor in patients with acute myocardial infarction: a randomized controlled trial. *JAMA*. 2006;295(9):1003-1010.
- Oishi A, Otani A, Sasahara M, et al. Granulocyte colony-stimulating factor protects retinal photoreceptor cells against light-induced damage. *Invest Ophthalmol Vis Sci*. 2008;49(12):5629-5635.
- Bussolino F, Wang JM, Defilippi P, et al. Granulocyte- and granulocyte-macrophage-colony stimulating factors induce human endothelial cells to migrate and proliferate. *Nature*. 1989;337(6206):471-473.
- Bussolino F, Ziche M, Wang JM, et al. In vitro and in vivo activation of endothelial cells by colony-stimulating factors. *J Clin Invest*. 1991;87(3):986-995.
- Lewis JL, Marley SB, Ojo M, et al. Opposing effects of PI3 kinase pathway activation on human myeloid and erythroid progenitor cell proliferation and differentiation in vitro. *Exp Hematol*. 2004;32(1):36-44.
- Li ZX, Li QY, Qiao J, et al. Granulocyte-colony stimulating factor is involved in low-dose LPS-induced neuroprotection. *Neurosci Lett*. 2009;465(2):128-132.
- Cuda G, Paternò R, Ceravolo R, et al. Protection of human endothelial cells from oxidative stress: role of Ras-ERK1/2 signaling. *Circulation*. 2002;105(8):968-974.
- O'Connor JC, Wallace DM, O'Brien CJ, Cotter TG. A novel antioxidant function for the tumor-suppressor gene p53 in the retinal ganglion cell. *Invest Ophthalmol Vis Sci*. 2008;49(10):4237-4244.
- Smith LE, Wesolowski E, McLellan A, et al. Oxygen-induced retinopathy in the mouse. *Invest Ophthalmol Vis Sci*. 1994;35(1):101-111.
- Schneider A, Kruger C, Steigleder T, et al. The hematopoietic factor G-CSF is a neuronal ligand that counteracts programmed cell death and drives neurogenesis. *J Clin Invest*. 2005;115(8):2083-2098.
- Sasahara M, Otani A, Oishi A, et al. Activation of bone marrow-derived microglia promotes photoreceptor survival in inherited retinal degeneration. *Am J Pathol*. 2008;172(6):1693-1703.
- Otani A, Kinder K, Ewalt K, Otero FJ, Schimmel P, Friedlander M. Bone marrow-derived stem cells target retinal astrocytes and can promote or inhibit retinal angiogenesis. *Nat Med*. 2002;8(9):1004-1010.
- Ritter MR, Banin E, Moreno SK, Aguilar E, Dorrell MI, Friedlander M. Myeloid progenitors differentiate into microglia and promote vascular repair in a model of ischemic retinopathy. *J Clin Invest*. 2006;116(12):3266-3276.
- Harada M, Qin Y, Takano H, et al. G-CSF prevents cardiac remodeling after myocardial infarction by activating the Jak-Stat pathway in cardiomyocytes. *Nat Med*. 2005;11(3):305-311.
- Avalos BR. Molecular analysis of the granulocyte colony-stimulating factor receptor. *Blood*. 1996;88(3):761-777.

Acknowledgments

This work was supported by the Ministry of Education, Science, Sports and Culture, Japan (grant-in-aid 17689045).

Authorship

Contribution: H.K. performed research, wrote the manuscript, and performed statistical analysis; A. Otani designed research, wrote the manuscript, and performed statistical analysis; A. Oishi performed research and analyzed and interpreted data; Y.M. and S.N. collected, analyzed, and interpreted data; and N.Y. analyzed and interpreted data.

Conflict-of-interest disclosure: The authors declare no competing financial interests.

Correspondence: Atsushi Otani, Department of Ophthalmology, Kyoto University Graduate School of Medicine, 54-Kawaharacho, Shyogoin, Sakyo-ku, Kyoto 606-8507, Japan; e-mail: otan@kuhp.kyoto-u.ac.jp.

32. Demetri GD. Granulocyte colony-stimulating factor and its receptor. *Blood*. 1991;78(11):2791-2808.
33. Huang HY, Lin SZ, Kuo JS, Chen WF, Wang MJ. G-CSF protects dopaminergic neurons from 6-OHDA induced toxicity via the ERK pathway. *Neurobiol Aging*. 2007;28(8):1258-1269.
34. Penn JS. Oxygen-induced retinopathy in the rat: possible contribution of peroxidation reactions. *Doc Ophthalmol*. 1990;74(3):179-186.
35. Phelps DL, Rosenbaum AL. Vitamin E in kitten oxygen-induced retinopathy: II. Blockage of vitreal neovascularization. *Arch Ophthalmol*. 1979;97(8):1522-1526.
36. Penn JS, Tolman BL, Lowery LA. Variable oxygen exposure causes preretinal neovascularization in the newborn rat. *Invest Ophthalmol Vis Sci*. 1993;34(3):576-585.
37. Fulton AB, Hansen RM, Petersen RA. The rod photoreceptors in retinopathy of prematurity: an electroretinographic study. *Arch Ophthalmol*. 2001;119(4):499-505.
38. Reisner DS, Hansen RM, Findl O, Petersen RA, Fulton AB. Dark-adapted thresholds in children with histories of mild retinopathy of prematurity. *Invest Ophthalmol Vis Sci*. 1997;38(6):1175-1183.
39. Tzekov R, Arden GB. The electroretinogram in diabetic retinopathy. *Surv Ophthalmol*. 1999;44(1):53-60.
40. Dembinska O, Rojas LM, Varma DR, Chemtob S, Lachapelle P. Graded contribution of retinal maturation to the development of oxygen-induced retinopathy in rats. *Invest Ophthalmol Vis Sci*. 2001;42(5):1111-1118.
41. Minatoguchi S, Takemura G, Chen XH, et al. Acceleration of the healing process and myocardial regeneration may be important as a mechanism of improvement of cardiac function and remodeling by postinfarction granulocyte colony-stimulating factor treatment. *Circulation*. 2004;109(21):2572-2580.
42. Ince H, Petzsch M, Kleine HD, et al. Preservation from left ventricular remodeling by front-integrated revascularization and stem cell liberation in evolving acute myocardial infarction by use of granulocyte-colony-stimulating factor (FIRST-LINE-AMI). *Circulation*. 2005;112(20):3097-3106.
43. Valgimigli M, Rigolin GM, Cittanti C, et al. Use of granulocyte-colony stimulating factor during acute myocardial infarction to enhance bone marrow stem cell mobilization in humans: clinical and angiographic safety profile. *Eur Heart J*. 2005;26(18):1838-1845.
44. Shimoji K, Yuasa S, Onizuka T, et al. G-CSF promotes the proliferation of developing cardiomyocytes in vivo and in derivation from ESCs and iPSCs. *Cell Stem Cell*. 2010;6(3):227-237.
45. Wen R, Cheng T, Song Y, et al. Continuous exposure to bright light up-regulates bFGF and CNTF expression in the rat retina. *Curr Eye Res*. 1998;17(5):494-500.